International Journal of Heat and Mass Transfer 52 (2009) 4769–4777

Contents lists available at ScienceDirect

International Journal of Heat and Mass Transfer

journal homepage: www.elsevier.com/locate/ijhmt

Asymptotic solution of thermocapillary convection in thin annular two-layer system with upper free surface

You-Rong Li *, Shuang-Cheng Wang, Shuang-Ying Wu, Lan Peng

College of Power Engineering, Chongqing University, Chongqing 400044, China

ARTICLE INFO

Article history:
Received 24 November 2008
Received in revised form 10 June 2009
Accepted 12 June 2009
Available online 18 July 2009

Keywords:
Thermocapillary flow
Two-layer system
Asymptotic solution

ABSTRACT

The steady laminar two-dimensional thermocapillary convection in the thin annular two superposed horizontal liquid layers with one free surface, one liquid/liquid interface subjected to a radial temperature gradient was investigated using asymptotical analysis. The pool is heated from the outer cylindrical wall and cooled at the inner wall. Bottom and top surfaces are adiabatic. The asymptotic solution is obtained in the core region in the limit as the aspect ratio, which is defined as the ratio of the lower layer thickness to the gap width, goes to zero. The numerical experiments are also carried out to compare with the asymptotic solution of the steady two-dimensional thermocapillary convection. The asymptotic results indicate that the expressions of velocity and temperature fields in the core region are valid in the limit of the small aspect ratio.

1. Introduction

There has been recently an increasing interest in the study of thermocapillary flows in a two-layer liquid system induced by horizontal temperature gradients, especially in microgravity-related fluid science and semiconductor crystal growth. In crystal growth, liquid-encapsulated crystal (LEC) growth is used to minimize evaporation of the volatile component from the melt and avoid crystallographic defects and degradation of electronic properties of the resulting products. The LEC growth process generates thermocapillary convective cells in the region of crystallization, which requires better understanding and controlling. Therefore, it has attracted great attention [1–3].

In the past, most studies about Rayleigh–Bénard convection in two immiscible liquids have been devoted to vertical heating [4–9]. Only few contributions were found to deal with a horizontal temperature gradient. Villers and Platten [10,11] studied experimentally thermal convection in two superposed immiscible fluid layers in a rectangular cavity with differentially heated end walls, and measured the horizontal velocity profiles in each layer as a function of the height. They also developed a simple theoretical model to calculate the horizontal velocity profile as a function of the ratio of viscosities, expansion coefficients, and thicknesses of both layers. Doi and Koster [12] studied theoretically the thermocapillary convection under microgravity conditions in two immiscible liquid layers with an upper free surface. An analytical solution was introduced for infinite horizontal layers, and four different flow profiles and three "halt" conditions which prevent the flow motion in the lower layer were found. Moreover, they carried out numerical simulations in a two-dimensional cavity in order to analyze the effect of the vertical walls. Then, Liu et al. [13,14] performed numerical simulations to investigate the thermogravitational and thermocapillary convection in a cavity containing two superposed immiscible liquid layers. They discovered that convective patterns depended on the property ratios of the two liquid layers and the thickness fractions of the layers, and also introduced an asymptotic solution for the velocity in the limit of infinite aspect ratio. Nepomnyashchy et al. [15] investigated numerically three-dimensional spiral thermocapillary flows of a two-layer fluid system filling a channel with a rectangular cross section. Steady and oscillatory thermocapillary motions and transitions between them were confirmed. Furthermore, Madruga et al. [16] studied the linear stability of two superposed horizontal liquid layers bounded by two solid planes and subjected to a horizontal temperature gradient. Four different flow patterns and temperature profiles were displayed for the basic state. A linear perturbative analysis with respect to bidimensional and three-dimensional perturbations revealed the existence of three kinds of patterns: wave propagation from the cold to the hot regions, waves propagating in the opposite direction or still stationary longitudinal rolls. Nepomnyashchy and Simanovskii [17] investigated the nonlinear stability of the same two-layer systems as Madruga et al. Periodic boundary conditions and heat-insulated lateral walls were considered, and it was concluded that the direction of the wave propagation depended on the ratio of the layers thicknesses and the Marangoni number. At the same time, Gupta et al. [18,19] performed computational studies of thermocapillary convection in

* Corresponding author. Tel.: +86 23 6511 2284; fax: +86 23 6510 2473.
E-mail address: liyourong@cqu.edu.cn (Y.-R. Li).

0017-9310/$ - see front matter © 2009 Elsevier Ltd. All rights reserved.
doi:10.1016/j.ijheatmasstransfer.2009.06.010

the absence of gravity within a differentially heated rectangular cavity containing two immiscible liquid layers. Interface deformations were considered in the study. They pointed out that the flow pattern in the encapsulated layer was strongly dependent on both the thickness and the viscosity of the encapsulant layer, and choosing an encapsulant with a greater sensitivity of interfacial tension to temperature could almost suppress thermocapillary convection in the melt. Recently, results of nonlinear simulations of purely thermocapillary and buoyancy-thermocapillary convective flows in two-layer systems in different scales under the action of a temperature gradient along the interface have been presented by Nepomnyashchy and Simanovskii [20]. They also conducted the nonlinear development of the instability in ultra-thin films caused by intermolecular forces. Chang et al. [21] investigated the interplay between buoyancy-induced and surface tension-driven convection in a two-layer liquid system in a cubic cavity using a hybrid thermal multiphase lattice Boltzmann method. They argued that the flow pattern in a two-layer fluid system with density inversion and heated from the sidewalls is qualitatively and quantitatively different from that in a two-layer case for which both the densities of fluids decrease linearly with temperature.

In theoretical investigations of thermocapillary convection, asymptotic or analytical solutions are of significance. Many asymptotic or analytical solutions play key roles in the early development of thermocapillary convection. Besides the theoretical meaning, asymptotic or analytical solutions can also be used to check the accuracy, convergence and effectiveness of various numerical computation methods and to improve their differencing schemes, grid generation ways and so on. The asymptotic or analytical solutions are, therefore, very useful even for the newly rapidly developing computational fluid dynamics. Cormack et al. [22] used asymptotic analysis to investigate natural convection in a single layer in a shallow rectangular cavity due to differentially heated end walls. They divided the flow into a central core region and two end regions, and found that in the core region the flow is parallel with fluid travelling from the hot end wall towards the cold end wall in the upper half of the cavity and fluid travelling in the opposite direction in the lower half of the cavity. Subsequently, Merker and Leal [23] examined natural convection in shallow cylindrical annuli. And Leppinen [24] indicated the disadvantage of the assumptions made by Merker and Leal and presented a revised version of the asymptotic analysis for natural convection in shallow cylindrical annuli. Sen and Davis [25] used the similar method to investigate thermocapillary convection in a single layer in a rectangular cavity with the free surface. Recently, we have reported an asymptotic solution of thermocapillary convection in a thin annular pool of silicon melt [26]. The purpose of this paper is to use asymptotic analysis to examine thermocapillary convection in thin annular two superposed horizontal liquid layers subjected to a radial temperature gradient.

2. Mathematical model

We analyze thermocapillary convection of the two immiscible liquid layers in a thin annular pool as shown schematically in Fig. 1. The thicknesses of the lower layer and the upper one are h_1 and h_2, respectively. The ratio of thickness is defined by $h^* = h_2/h_1$. The radius of the inner cylinder is r_i; and the radius of the outer cylinder is $r_o = r_i + l$. The pool has a free upper surface and solid bottom. The aspect ratio of pool is $\varepsilon = h_1/l$. For the thin pools, $\varepsilon \to 0$, a measure of curvature in the annular gap is given by $\Gamma = r_i/l$. A third geometric parameter of the pool is $\delta = r_i/h_1$ which is related to ε and Γ by $\Gamma = \varepsilon\delta$.

The inner and outer cylinders maintain at constant temperatures T_c and T_h ($T_h > T_c$), respectively. The horizontal temperature gradient varies in the radial direction. The thermocapillary convection is generated by the surface tension gradient on the top free surface. The following assumptions are introduced in our model: (1) The two layers are incompressible Newtonian fluids and a constant property assumption is applicable except for the surface tension. (2) The velocity is small and the flow is the two-dimensional steady laminar. (3) Both the free surface and the interface are flat and nondeformable [11]. (4) On the top free surface and interface, the thermocapillary force is taken into account. At other solid–liquid boundaries, the no-slip condition is applied. (5) Both bottom and top boundaries are assumed to be adiabatic.

With the above assumptions, the steady-state governing equations in cylindrical coordinate are expressed as follows:

$$\frac{1}{r}\frac{\partial}{\partial r}(ru_i) + \frac{\partial v_i}{\partial z} = 0, \tag{1}$$

$$u_i\frac{\partial u_i}{\partial r} + v_i\frac{\partial u_i}{\partial z} = -\frac{1}{\rho_i}\frac{\partial p_i}{\partial r} + \nu_i\left(\frac{\partial^2 u_i}{\partial r^2} + \frac{1}{r}\frac{\partial u_i}{\partial r} - \frac{u_i}{r^2} + \frac{\partial^2 u_i}{\partial z^2}\right), \tag{2}$$

$$u_i\frac{\partial v_i}{\partial r} + v_i\frac{\partial v_i}{\partial z} = -\frac{1}{\rho_i}\frac{\partial p_i}{\partial z} + \nu_i\left(\frac{\partial^2 v_i}{\partial r^2} + \frac{1}{r}\frac{\partial v_i}{\partial r} + \frac{\partial^2 v_i}{\partial z^2}\right), \tag{3}$$

$$u_i\frac{\partial T_i}{\partial r} + v_i\frac{\partial T_i}{\partial z} = \alpha_i\left(\frac{\partial^2 T_i}{\partial r^2} + \frac{1}{r}\frac{\partial T_i}{\partial r} + \frac{\partial^2 T_i}{\partial z^2}\right), \tag{4}$$

where the subscript $i = 1,\ 2$ refers to the lower layer and the upper one, u and v are the radial and axial velocities, r and z are the cylindrical coordinates, respectively. ρ is the density, p is the pressure, ν is the kinematic viscosity, and α is the thermal diffusivity.

The boundary conditions are:

$$u_1 = v_1 = 0, \quad \frac{\partial T_1}{\partial z} = 0 \quad \text{at } z = -h_1, \tag{5}$$

$$u_1 = u_2, \quad v_1 = v_2 = 0, \quad T_1 = T_2, \quad \lambda_1\frac{\partial T_1}{\partial z} = \lambda_2\frac{\partial T_2}{\partial z},$$
$$\mu_1\frac{\partial u_1}{\partial z} - \mu_2\frac{\partial u_2}{\partial z} = -\gamma_{T,1}\frac{\partial T_1}{\partial r} \quad \text{at } z = 0, \tag{6}$$

$$v_2 = 0, \quad \mu_2\frac{\partial u_2}{\partial z} = -\gamma_{T,2}\frac{\partial T_2}{\partial r}, \quad \frac{\partial T_2}{\partial z} = 0 \quad \text{at } z = h_2, \tag{7}$$

$$u_i = v_i = 0, \quad T = T_c \quad \text{at } r = r_i, \tag{8}$$

$$u_i = v_i = 0, \quad T = T_h \text{ at } \quad r = r_o, \tag{9}$$

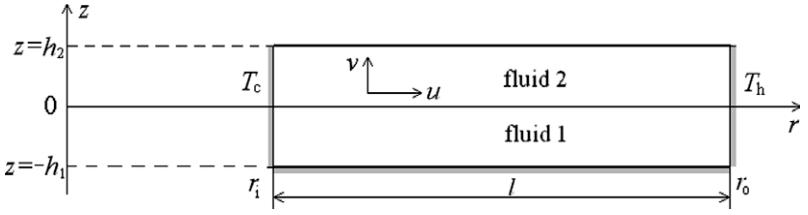

Fig. 1. Physical model.

where $\gamma_{T,1}$ is the interface tension temperature coefficient between liquid 1 and liquid 2, $\gamma_{T,2}$ is surface tension temperature coefficient of liquid 2, λ is the thermal conductivity, μ is the dynamic viscosity.

Eqs. (1)–(4) are nondimensionalized using

$$R=\frac{r}{h_1},\quad Z=\frac{z}{h_1},\quad \theta=\frac{T-T_c}{T_h-T_c},\quad P=\frac{ph_1^2}{\rho_1 v_1^2}\quad \text{and}\quad (U,V)=(u,v)\frac{h_1}{\varepsilon v_1},$$

where θ is the nondimensional temperature. With the introduction of the axisymmetric stream function ψ, and vorticity ω, defined by the relations

$$\omega=\frac{\partial U}{\partial Z}-\frac{\partial V}{\partial R},\quad U=-\frac{1}{R}\frac{\partial \psi}{\partial Z}\quad \text{and}\quad V=\frac{1}{R}\frac{\partial \psi}{\partial R}. \tag{10}$$

The governing equations can be reduced to

$$\frac{\varepsilon}{R}\left(\frac{\partial \psi_i}{\partial R}\frac{\partial \omega_i}{\partial Z}-\frac{\partial \psi_i}{\partial Z}\frac{\partial \omega_i}{\partial R}+\frac{\omega_i}{R}\frac{\partial \psi_i}{\partial Z}\right)=\frac{v_i}{v_1}\left(\frac{\partial^2\omega_i}{\partial R^2}+\frac{1}{R}\frac{\partial \omega_i}{\partial R}-\frac{\omega_i}{R^2}+\frac{\partial^2\omega_i}{\partial Z^2}\right), \tag{11}$$

$$\frac{1}{R}\frac{\partial^2\psi_i}{\partial R^2}-\frac{1}{R^2}\frac{\partial \psi_i}{\partial R}+\frac{1}{R}\frac{\partial^2\psi_i}{\partial Z^2}=-\omega_i, \tag{12}$$

$$\frac{Pr\varepsilon}{R}\left(\frac{\partial \psi_i}{\partial R}\frac{\partial \theta_i}{\partial Z}-\frac{\partial \psi_i}{\partial Z}\frac{\partial \theta_i}{\partial R}\right)=\frac{\alpha_i}{\alpha_1}\left(\frac{\partial^2\theta_i}{\partial R^2}+\frac{1}{R}\frac{\partial \theta_i}{\partial R}+\frac{\partial^2\theta_i}{\partial Z^2}\right). \tag{13}$$

The nondimensional boundary conditions are:

$$\psi_1=\frac{\partial \psi_1}{\partial Z}=\frac{\partial \theta_1}{\partial Z}=0\quad \text{at } Z=-1, \tag{14}$$

$$\psi_1=\psi_2=0,\quad \frac{\partial \psi_1}{\partial Z}=\frac{\partial \psi_2}{\partial Z},\quad \theta_1=\theta_2,$$
$$\frac{\partial \theta_1}{\partial Z}=\lambda^*\frac{\partial \theta_2}{\partial Z},\quad \frac{1}{R}\left(\frac{\partial^2\psi_1}{\partial Z^2}-\mu^*\frac{\partial^2\psi_2}{\partial Z^2}\right)=Re\frac{\partial \theta_1}{\partial R}\quad \text{at } Z=0, \tag{15}$$

$$\psi_2=\frac{\partial \theta_2}{\partial Z}=0,\quad \frac{\mu^*}{R}\frac{\partial^2\psi_2}{\partial Z^2}=\gamma_T^* Re\frac{\partial \theta_2}{\partial R}\quad \text{at } Z=h^*, \tag{16}$$

$$\psi_i=\frac{\partial \psi_i}{\partial R}=0,\quad \theta_i=0\quad \text{at } R=\delta, \tag{17}$$

$$\psi_i=\frac{\partial \psi_i}{\partial R}=0,\quad \theta_i=1\quad \text{at } R=\delta+\frac{1}{\varepsilon}. \tag{18}$$

In the above, Pr is the Prandtl number defined by $Pr=\nu_1/\alpha_1$, Re is the thermocapillary Reynolds number defined by $Re=\gamma_{T,1}l(T_h-T_c)/(\nu_1\mu_1)$. μ^*, γ_T^* and λ^* are the ratios of dynamic viscosity, surface tension temperature coefficient and thermal conductivity of both liquids: $\mu^*=\mu_2/\mu_1,\ \gamma_T^*=\gamma_T,\ 2\gamma_T,\ 1,\ \lambda^*=\lambda_2/\lambda_1$. The strength of thermocapillary convection is also characterized by the Marangoni number, $Ma=\gamma_{T,1}l(T_h-T_c)/(\mu_1 a_1)$. The Marangoni numbers defined above may be expressed as the product of the Prandtl number and a thermocapillary Reynolds number, i.e. $Ma=RePr$.

The solutions of Eqs. (11)–(13) subjected to boundary conditions (14)–(18) will be obtained in the asymptotic limit as $\varepsilon\to 0$ with both Pr and Re fixed. In this model, Γ is of O(1). Therefore, the radial coordinate R is of $O(1/\varepsilon)$ throughout the entire annular pool. It is convenient to make the transformation $R=\delta+X$, so that $1/R=1/(\delta+X)=\varepsilon/(\Gamma+\varepsilon X)$ with X varying from $X=0$ at the inner cylinder to $X=1/\varepsilon$ at the outer cylinder. The transformed equations become

$$\frac{\varepsilon^2}{\Gamma+\varepsilon X}\left(\frac{\partial \psi_i}{\partial X}\frac{\partial \omega_i}{\partial Z}-\frac{\partial \psi_i}{\partial Z}\frac{\partial \omega_i}{\partial X}+\frac{\varepsilon\omega_i}{\Gamma+\varepsilon X}\frac{\partial \psi_i}{\partial Z}\right)=\frac{v_i}{v_1}\left(\frac{\partial^2\omega_i}{\partial X^2}+\frac{\varepsilon}{\Gamma+\varepsilon X}\frac{\partial \omega_i}{\partial X}-\frac{\varepsilon^2\omega_i}{(\Gamma+\varepsilon X)^2}+\frac{\partial^2\omega_i}{\partial Z^2}\right), \tag{19}$$

$$\frac{\varepsilon}{\Gamma+\varepsilon X}\left(\frac{\partial^2\psi_i}{\partial X^2}-\frac{\varepsilon}{\Gamma+\varepsilon X}\frac{\partial \psi_i}{\partial X}+\frac{\partial^2\psi_i}{\partial Z^2}\right)=-\omega_i, \tag{20}$$

$$\frac{Pr\varepsilon^2}{\Gamma+\varepsilon X}\left(\frac{\partial \psi_i}{\partial X}\frac{\partial \theta_i}{\partial Z}-\frac{\partial \psi_i}{\partial Z}\frac{\partial \theta_i}{\partial X}\right)=\frac{\alpha_i}{\alpha_1}\left(\frac{\partial^2\theta_i}{\partial X^2}+\frac{\varepsilon}{\Gamma+\varepsilon X}\frac{\partial \theta_i}{\partial X}+\frac{\partial^2\theta_i}{\partial Z^2}\right). \tag{21}$$

3. Core region solutions

In the core region, the radial changes occur over distances of $O(1/\varepsilon)$, which suggests the introduction of a core variable $\hat{X}=\varepsilon X$. If θ and ω are denoted by $\hat{\theta}$ and $\hat{\omega}$, respectively, and the rescaling $\hat{\psi}=\varepsilon\psi$ has been used to ensure a balance at leading order in the stream function equation in the core, the governing equations become

$$\frac{\varepsilon^2}{\Gamma+\hat{X}}\left(\frac{\partial \hat{\psi}_i}{\partial \hat{X}}\frac{\partial \hat{\omega}_i}{\partial Z}-\frac{\partial \hat{\psi}_i}{\partial Z}\frac{\partial \hat{\omega}_i}{\partial \hat{X}}+\frac{\hat{\omega}_i}{\Gamma+\hat{X}}\frac{\partial \hat{\psi}_i}{\partial Z}\right)=\varepsilon^2\frac{v_i}{v_1}\left[\frac{\partial^2\hat{\omega}_i}{\partial \hat{X}^2}+\frac{1}{\Gamma+\hat{X}}\frac{\partial \hat{\omega}_i}{\partial \hat{X}}-\frac{\hat{\omega}_i}{(\Gamma+\hat{X})^2}\right]+\frac{v_i}{v_1}\frac{\partial^2\hat{\omega}_i}{\partial Z^2}, \tag{22}$$

$$\frac{1}{\Gamma+\hat{X}}\frac{\partial^2\hat{\psi}_i}{\partial Z^2}+\frac{\varepsilon^2}{\Gamma+\hat{X}}\left(\frac{\partial^2\hat{\psi}_i}{\partial \hat{X}^2}-\frac{1}{\Gamma+\hat{X}}\frac{\partial \hat{\psi}_i}{\partial \hat{X}}\right)=-\hat{\omega}_i, \tag{23}$$

$$\frac{Pr\varepsilon^2}{\Gamma+\hat{X}}\left(\frac{\partial \hat{\psi}_i}{\partial \hat{X}}\frac{\partial \hat{\theta}_i}{\partial Z}-\frac{\partial \hat{\psi}_i}{\partial Z}\frac{\partial \hat{\theta}_i}{\partial \hat{X}}\right)=\frac{\alpha_i}{\alpha_1}\frac{\partial^2\hat{\theta}_i}{\partial Z^2}+\varepsilon^2\frac{\alpha_i}{\alpha_1}\left(\frac{\partial^2\hat{\theta}_i}{\partial \hat{X}^2}+\frac{1}{\Gamma+\hat{X}}\frac{\partial \hat{\theta}_i}{\partial \hat{X}}\right). \tag{24}$$

The nondimensional boundary conditions are

$$\hat{\psi}_1=\frac{\partial \hat{\psi}_1}{\partial Z}=\frac{\partial \hat{\theta}_1}{\partial Z}=0\quad \text{at } Z=-1, \tag{25}$$

$$\hat{\psi}_1=\hat{\psi}_2=0,\quad \frac{\partial \hat{\psi}_1}{\partial Z}=\frac{\partial \hat{\psi}_2}{\partial Z},\quad \hat{\theta}_1=\hat{\theta}_2,\quad \frac{\partial \hat{\theta}_1}{\partial Z}=\lambda^*\frac{\partial \hat{\theta}_2}{\partial Z},$$
$$\frac{1}{\Gamma+\hat{X}}\left(\frac{\partial^2\hat{\psi}_1}{\partial Z^2}-\mu^*\frac{\partial^2\hat{\psi}_2}{\partial Z^2}\right)=Re\varepsilon\frac{\partial \hat{\theta}_1}{\partial \hat{X}}\quad \text{at } Z=0, \tag{26}$$

$$\hat{\psi}_2=\frac{\partial \hat{\theta}_2}{\partial Z}=0,\quad \frac{\mu^*}{\Gamma+\hat{X}}\frac{\partial^2\hat{\psi}_2}{\partial Z^2}=\gamma_T^* Re\varepsilon\frac{\partial \hat{\theta}_2}{\partial \hat{X}}\quad \text{at } Z=h^*. \tag{27}$$

A solution to these equations is sought out using a regular asymptotic expansion of the form

$$(\hat{\theta}_i,\hat{\psi}_i,\hat{\omega}_i)=\sum_{j=0}^{N}\varepsilon^j(\hat{\theta}_{ij},\hat{\psi}_{ij},\hat{\omega}_{ij}). \tag{28}$$

Substituting expansion (28) into Eqs. (22)–(27), we have

$$\frac{\partial^2\hat{\omega}_{i0}}{\partial Z^2}=0, \tag{29}$$

$$\frac{1}{\Gamma+\hat{X}}\frac{\partial^2\hat{\psi}_{i0}}{\partial Z^2}=-\hat{\omega}_{i0}, \tag{30}$$

$$\frac{\partial^2\hat{\theta}_{i0}}{\partial Z^2}=0. \tag{31}$$

The boundary conditions are

$$\hat{\psi}_{10}=\frac{\partial \hat{\psi}_{10}}{\partial Z}=\frac{\partial \hat{\theta}_{10}}{\partial Z}=0\quad \text{at } Z=-1, \tag{32}$$

$$\hat{\psi}_{10}=\hat{\psi}_{20}=0,\quad \frac{\partial\hat{\psi}_{10}}{\partial Z}=\frac{\partial\hat{\psi}_{20}}{\partial Z},\quad \hat{\theta}_{10}=\hat{\theta}_{20},$$
$$\frac{\partial\hat{\theta}_{10}}{\partial Z}=\lambda^*\frac{\partial\hat{\theta}_{20}}{\partial Z},\quad \frac{\partial^2\hat{\psi}_{10}}{\partial Z^2}-\mu^*\frac{\partial^2\hat{\psi}_{20}}{\partial Z^2}=0\quad \text{at } Z=0, \tag{33}$$

$$\hat{\psi}_{20}=\frac{\partial\hat{\theta}_{20}}{\partial Z}=0,\quad \frac{\partial^2\hat{\psi}_{20}}{\partial Z^2}=0\quad \text{at } Z=h^*. \tag{34}$$

The solutions to Eqs. (29)–(31) are

$$\hat{\theta}_{i0}=f_{i0}(\widehat{X},\Gamma)Z+g_{i0}(\widehat{X},\Gamma), \tag{35}$$

$$\hat{\omega}_{i0}=f'_{i0}(\widehat{X},\Gamma)Z+g'_{i0}(\widehat{X},\Gamma), \tag{36}$$

$$\hat{\psi}_{i0}=h_{i0}(\widehat{X},\Gamma)Z+k_{i0}(\widehat{X},\Gamma)-(\Gamma+\widehat{X})\left[f'_{i0}(\widehat{X},\Gamma)\frac{Z^3}{6}+g'_{i0}(\widehat{X},\Gamma)\frac{Z^2}{2}\right]. \tag{37}$$

According to the boundary conditions, there are

$$f_{i0}(\widehat{X},\Gamma)=h_{i0}(\widehat{X},\Gamma)=k_{i0}(\widehat{X},\Gamma)=f'_{i0}(\widehat{X},\Gamma)=g'_{i0}(\widehat{X},\Gamma)=0. \tag{38}$$

Hence, at O(1), the solutions are

$$\hat{\psi}_{i0}=\hat{\omega}_{i0}=0, \tag{39}$$
$$\hat{\theta}_{i0}=g_{i0}(\widehat{X},\Gamma). \tag{40}$$

At O(ε) the governing equations are identical to those at O(1). Thus the solutions are given by Eqs. (35)–(37) with the subscript 0 replaced everywhere by 1.

The boundary conditions are

$$\hat{\psi}_{11}=\frac{\partial\hat{\psi}_{11}}{\partial Z}=\frac{\partial\hat{\theta}_{11}}{\partial Z}=0\quad \text{at } Z=-1, \tag{41}$$

$$\hat{\psi}_{11}=\hat{\psi}_{21}=0,\quad \frac{\partial\hat{\psi}_{11}}{\partial Z}=\frac{\partial\hat{\psi}_{21}}{\partial Z},\quad \hat{\theta}_{11}=\hat{\theta}_{21},\quad \frac{\partial\hat{\theta}_{11}}{\partial Z}=\lambda^*\frac{\partial\hat{\theta}_{21}}{\partial Z},$$
$$\frac{1}{\Gamma+\widehat{X}}\left(\frac{\partial^2\hat{\psi}_{11}}{\partial Z^2}-\mu^*\frac{\partial^2\hat{\psi}_{21}}{\partial Z^2}\right)=Re\frac{\partial\hat{\theta}_{10}}{\partial\widehat{X}}\quad \text{at } Z=0, \tag{42}$$

$$\hat{\psi}_{21}=\frac{\partial\hat{\theta}_{21}}{\partial Z}=0,\quad \frac{\mu^*}{\Gamma+\widehat{X}}\frac{\partial^2\hat{\psi}_{21}}{\partial Z^2}=Re\gamma_T^*\frac{\partial\hat{\theta}_{20}}{\partial\widehat{X}}\quad \text{at } Z=h^*. \tag{43}$$

The solutions which satisfy the boundary conditions are

$$\hat{\psi}_{11}=-c_{11}\left(\frac{Z^3}{6}+\frac{Z^2}{3}+\frac{Z}{6}\right), \tag{44}$$

$$\hat{\psi}_{21}=-c_{11}\left(\frac{AZ^3}{6}+\frac{BZ^2}{2}+\frac{Z}{6}\right), \tag{45}$$

$$\hat{\omega}_{11}=\frac{c_{11}}{\Gamma+\widehat{X}}\left(Z+\frac{2}{3}\right), \tag{46}$$

$$\hat{\omega}_{21}=\frac{c_{11}}{\Gamma+\widehat{X}}(AZ+B), \tag{47}$$

$$\frac{\partial\hat{\theta}_{i0}}{\partial\widehat{X}}=\frac{3\mu^*+4h^*}{3\gamma_T^*h^*-6h^*}\frac{1}{Re}\frac{c_{11}}{\Gamma+\widehat{X}}, \tag{48}$$

$$\theta_{11}=\theta_{21}=g_{11}(\widehat{X},\Gamma), \tag{49}$$

where $A=\frac{\gamma_T^*\mu^*+2\gamma_T^*h^*+\mu^*}{2\mu^*h^{*2}-\gamma_T^*\mu^*h^{*2}}$, $B=\frac{2\gamma_T^*h^*+3\mu^*}{3\gamma_T^*\mu^*h^*-6\mu^*h^*}$ and c_{11} is an undetermined function of $\widehat{X}$.

At O(ε^2) the energy equation is

$$\frac{Pr}{\Gamma+\widehat{X}}\left(\frac{\partial\hat{\psi}_{i0}}{\partial\widehat{X}}\frac{\partial\hat{\theta}_{i0}}{\partial Z}-\frac{\partial\hat{\psi}_{i0}}{\partial Z}\frac{\partial\hat{\theta}_{i0}}{\partial\widehat{X}}\right)=\frac{\alpha_i}{\alpha_1}\left(\frac{\partial^2\hat{\theta}_{i2}}{\partial Z^2}+\frac{\partial^2\hat{\theta}_{i0}}{\partial\widehat{X}^2}+\frac{1}{\Gamma+\widehat{X}}\frac{\partial\hat{\theta}_{i0}}{\partial\widehat{X}}\right), \tag{50}$$

which, upon substitution of the O(1) solution, becomes

$$\frac{\partial^2\hat{\theta}_{i2}}{\partial Z^2}+\frac{3\mu^*+4h^*}{3\gamma_T^*h^*-6h^*}\frac{1}{Re}\frac{1}{\Gamma+\widehat{X}}\frac{\partial c_{11}}{\partial\widehat{X}}=0. \tag{51}$$

For liquid 1, the form of the equation is

$$\frac{\partial^2\hat{\theta}_{12}}{\partial Z^2}+\frac{3\mu^*+4h^*}{3\gamma_T^*h^*-6h^*}\frac{1}{Re}\frac{1}{\Gamma+\widehat{X}}\frac{\partial c_{11}}{\partial\widehat{X}}=0, \tag{52}$$

which is integrated from $Z=-1$ to $Z=0$ to give

$$\left.\frac{\partial\hat{\theta}_{12}}{\partial Z}\right|_{Z=0}=-\frac{3\mu^*+4h^*}{3\gamma_T^*h^*-6h^*}\frac{1}{\Gamma+\widehat{X}}\frac{1}{Re}\frac{\partial c_{11}}{\partial\widehat{X}}. \tag{53}$$

For liquid 2, the form of Eq. (51) becomes

$$\frac{\partial^2\hat{\theta}_{22}}{\partial Z^2}+\frac{3\mu^*+4h^*}{3\gamma_T^*h^*-6h^*}\frac{1}{Re}\frac{1}{\Gamma+\widehat{X}}\frac{\partial c_{11}}{\partial\widehat{X}}=0, \tag{54}$$

which is integrated from $Z=0$ to $Z=h^*$ to give

$$\left.\frac{\partial\hat{\theta}_{22}}{\partial Z}\right|_{Z=0}=\frac{3\mu^*+4h^*}{3\gamma_T^*h^*-6h^*}\frac{h^*}{\Gamma+\widehat{X}}\frac{1}{Re}\frac{\partial c_{11}}{\partial\widehat{X}}. \tag{55}$$

Combining Eqs. (53) and (55) and using the boundary condition at $Z=0$: $\partial\hat{\theta}_{12}/\partial Z=\lambda^*\partial\hat{\theta}_{22}/\partial Z$ yields

$$\frac{1}{\Gamma+\widehat{X}}\frac{\partial c_{11}}{\partial\widehat{X}}=0. \tag{56}$$

It shows that c_{11} is a constant and consequently Eq. (48) can be integrated to give

$$\hat{\theta}_{i0}=\frac{3\mu^*+4h^*}{3\gamma_T^*h^*-6h^*}\frac{c_{11}}{Re}\ln(\Gamma+\widehat{X})+c_{11}^*, \tag{57}$$

where both c_{11} and c_{11}^* are constants. They can be determined by matching the core solution with solutions in the end regions.

Repeating the above procedures at O(ε^2) and O(ε^3), we have

$$\hat{\psi}_{1j}=-c_{1j}\left(\frac{Z^3}{6}+\frac{Z^2}{3}+\frac{Z}{6}\right),\quad (j=2,3) \tag{58}$$

$$\hat{\psi}_{2j}=-c_{1j}\left(\frac{AZ^3}{6}+\frac{BZ^2}{2}+\frac{Z}{6}\right),\quad (j=2,3) \tag{59}$$

$$\hat{\omega}_{1j}=\frac{c_{1j}}{\Gamma+\widehat{X}}\left(Z+\frac{2}{3}\right),\quad (j=2,3) \tag{60}$$

$$\hat{\omega}_{2j}=\frac{c_{1j}}{\Gamma+\widehat{X}}(AZ+B),\quad (j=2,3) \tag{61}$$

$$\hat{\theta}_{1j-1}=\hat{\theta}_{2j-1}=\frac{3\mu^*+4h^*}{3\gamma_T^*h^*-6h^*}\frac{c_{1j}}{Re}\ln(\Gamma+\widehat{X})+c_{1j}^*,\quad (j=2,3) \tag{62}$$

where c_{1j} and c_{1j}^* are also numerical constants.

At O(ε^3) the energy equation is

$$\frac{Pr}{\Gamma+\widehat{X}}\left(\frac{\partial\hat{\psi}_{i1}}{\partial\widehat{X}}\frac{\partial\hat{\theta}_{i0}}{\partial Z}+\frac{\partial\hat{\psi}_{i0}}{\partial\widehat{X}}\frac{\partial\hat{\theta}_{i1}}{\partial Z}-\frac{\partial\hat{\psi}_{i1}}{\partial Z}\frac{\partial\hat{\theta}_{i0}}{\partial\widehat{X}}-\frac{\partial\hat{\psi}_{i0}}{\partial Z}\frac{\partial\hat{\theta}_{i1}}{\partial\widehat{X}}\right)$$
$$=\frac{\alpha_i}{\alpha_1}\left(\frac{\partial^2\hat{\theta}_{i3}}{\partial Z^2}+\frac{\partial^2\hat{\theta}_{i1}}{\partial\widehat{X}^2}+\frac{1}{\Gamma+\widehat{X}}\frac{\partial\hat{\theta}_{i1}}{\partial\widehat{X}}\right), \tag{63}$$

which, upon substitution of the O(1) and O(ε) solution, becomes

$$\frac{\partial^2\hat{\theta}_{13}}{\partial Z^2}=\frac{3\mu^*+4h^*}{3\gamma_T^*h^*-6h^*}\frac{c_{11}^2}{Re}\frac{Pr}{(\Gamma+\widehat{X})^2}\left(\frac{Z^2}{2}+\frac{2Z}{3}+\frac{1}{6}\right), \tag{64a}$$

$$\frac{\partial^2\hat{\theta}_{23}}{\partial Z^2}=\frac{3\mu^*+4h^*}{3\gamma_T^*h^*-6h^*}\frac{c_{11}^2}{Re}\frac{1}{\alpha^*}\frac{Pr}{(\Gamma+\widehat{X})^2}\left(\frac{AZ^2}{2}+BZ+\frac{1}{6}\right), \tag{64b}$$

where $\alpha^*=\alpha_2/\alpha_1$ is the ratio of thermal diffusivity of both liquids. These two equations are integrated twice respect to Z to give

$$\hat{\theta}_{13}=\frac{3\mu^*+4h^*}{3\gamma_T^*h^*-6h^*}\frac{c_{11}^2}{Re}\frac{Pr}{(\Gamma+\hat{X})^2}\left(\frac{Z^4}{24}+\frac{Z^3}{9}+\frac{Z^2}{12}\right)+\Theta_{13}(\hat{X}), \tag{65a}$$

$$\hat{\theta}_{23}=\frac{3\mu^*+4h^*}{3\gamma_T^*h^*-6h^*}\frac{1}{\alpha^*}\frac{c_{11}^2}{Re}\frac{Pr}{(\Gamma+\hat{X})^2}\left(\frac{AZ^4}{24}+\frac{BZ^3}{6}+\frac{Z^2}{12}\right)+\Theta_{23}(\hat{X}), \tag{65b}$$

where $\Theta_{13}(\hat{X})$ and $\Theta_{23}(\hat{X})$ are undetermined functions of $\hat{X}$. Using the boundary condition at $Z=0:\ \hat{\theta}_{13}=\hat{\theta}_{23}$ yields

$$\Theta_{13}(\hat{X})=\Theta_{23}(\hat{X}), \tag{66}$$

which can only be determined by examining the energy equation at $O(\varepsilon^5)$. Upon substitution of known values, the energy equation at $O(\varepsilon^5)$ is given by

$$\frac{\partial^2\hat{\theta}_{15}}{\partial Z^2}+\frac{4M}{(\Gamma+\hat{X})^4}\left(\frac{Z^4}{24}+\frac{Z^3}{9}+\frac{Z^2}{12}\right)+\frac{\partial^2\Theta_{13}}{\partial\hat{X}^2}+\frac{1}{\Gamma+\hat{X}}\frac{\partial\Theta_{13}}{\partial\hat{X}}=0, \tag{67a}$$

$$\frac{\partial^2\hat{\theta}_{25}}{\partial Z^2}+\frac{1}{\alpha^*}\frac{4M}{(\Gamma+\hat{X})^4}\left(\frac{AZ^4}{24}+\frac{BZ^3}{6}+\frac{Z^2}{12}\right)+\frac{\partial^2\Theta_{23}}{\partial\hat{X}^2}+\frac{1}{\Gamma+\hat{X}}\frac{\partial\Theta_{23}}{\partial\hat{X}}=0, \tag{67b}$$

where $M=\frac{3\mu^*+4h^*}{3\gamma_T^*h^*-6h^*}\frac{c_{11}^2Pr}{Re}$.

Integrating Eq. (67a) from $Z=-1$ to $Z=0$, and Eq. (67b) from $Z=0$ to $Z=h^*$, we have

$$\frac{\partial^2\Theta_{13}}{\partial\hat{X}^2}+\frac{1}{\Gamma+\hat{X}}\frac{\partial\Theta_{13}}{\partial\hat{X}}=-\frac{M}{30}\frac{1}{(\Gamma+\hat{X})^4}-\left.\frac{\partial\hat{\theta}_{15}}{\partial Z}\right|_{Z=0}, \tag{68a}$$

$$\frac{\partial^2\Theta_{23}}{\partial\hat{X}^2}+\frac{1}{\Gamma+\hat{X}}\frac{\partial\Theta_{23}}{\partial\hat{X}}=-\frac{M(3Ah^{*4}+15Bh^{*3}+10h^{*2})}{90}\frac{1}{\alpha^*}\times\frac{1}{(\Gamma+\hat{X})^4}+\frac{1}{h^*}\left.\frac{\partial\hat{\theta}_{25}}{\partial Z}\right|_{Z=0}. \tag{68b}$$

Combining Eqs. (68a) and (68b) and using the boundary condition at $Z=0:\ \partial\hat{\theta}_{15}/\partial Z=\lambda^*\partial\hat{\theta}_{25}/\partial Z$ yields

$$\frac{\partial^2\Theta_{13}}{\partial\hat{X}^2}+\frac{1}{\Gamma+\hat{X}}\frac{\partial\Theta_{13}}{\partial\hat{X}}=-\frac{M}{(\Gamma+\hat{x})^4}\times\left(\frac{\lambda^*h^*}{\lambda^*h^*+1}\frac{1}{\alpha^*}\frac{3Ah^{*4}+15Bh^{*3}+10h^{*2}}{90}+\frac{1}{\lambda^*h^*+1}\frac{1}{30}\right), \tag{69}$$

which can be integrated twice with respect to $\hat{X}$ to give

$$\Theta_{13}=a_3'\ln(\Gamma+\hat{X})+d_3-\left(\frac{1}{120}\frac{1}{\lambda^*h^*+1}+\frac{3Ah^{*4}+15Bh^{*3}+10h^{*2}}{360}\frac{\lambda^*h^*}{\lambda^*h^*+1}\frac{1}{\alpha^*}\right)\frac{M}{(\Gamma+\hat{X})^2}, \tag{70}$$

where a_3' and d_3 are constants, which must be determined by matching with the end region solutions.

4. End region solution

In the cold end region near the inner cylinder, θ, ψ and ω are denoted by $\bar{\theta}$, $\bar{\psi}$ and $\bar{\omega}$, while in the hot end region, $\tilde{\theta}$, $\tilde{\psi}$ and $\tilde{\omega}$ are used. Since the streamlines in the core are parallel at the leading order, they must eventually enter into the end regions. Hence $\bar{\psi}$ and $\tilde{\psi}$ must be rescaled as $\bar{\psi}=\varepsilon\psi$ and $\tilde{\psi}=\varepsilon\psi$. The governing equations in the cold end are Eqs. (19)–(21) while the governing equations in the hot end are obtained from them by performing the transformation $\xi=1/\varepsilon-X$.

In order to match the end region solutions with the solutions in the core region, the flow variables are expanded as

$$(\bar{\theta}_i,\bar{\psi}_i,\bar{\omega}_i,\tilde{\theta}_i,\tilde{\psi}_i,\tilde{\omega}_i)=\sum_{j=0}^{N}\varepsilon^j(\bar{\theta}_{ij},\bar{\psi}_{ij},\bar{\omega}_{ij},\tilde{\theta}_{ij},\tilde{\psi}_{ij},\tilde{\omega}_{ij}). \tag{71}$$

The matching conditions between the core and end region solutions are given by

$$\lim_{\hat{x}\to0}(\hat{\theta},\hat{\psi},\hat{\omega})_{core}\iff\lim_{x\to\infty}(\bar{\theta},\bar{\psi},\bar{\omega})_{cold}, \tag{72}$$

$$\lim_{\hat{x}\to1}(\hat{\theta},\hat{\psi},\hat{\omega})_{core}\iff\lim_{\xi\to\infty}(\tilde{\theta},\tilde{\psi},\tilde{\omega})_{hot}, \tag{73}$$

where the symbol $\iff$ is used to indicate the matching conditions applied in the limit as $\varepsilon\to0$.

At O(1), the governing equations in the cold end region are

$$\frac{\partial^2\bar{\omega}_{i0}}{\partial X^2}+\frac{\partial^2\bar{\omega}_{i0}}{\partial Z^2}=0, \tag{74}$$

$$-\frac{1}{\Gamma}\left(\frac{\partial^2\bar{\psi}_{i0}}{\partial X^2}+\frac{\partial^2\bar{\psi}_{i0}}{\partial Z^2}\right)=\bar{\omega}_{i0}, \tag{75}$$

$$\frac{\partial^2\bar{\theta}_{i0}}{\partial X^2}+\frac{\partial^2\bar{\theta}_{i0}}{\partial Z^2}=0. \tag{76}$$

When Eq. (76) is combined with the appropriate boundary conditions, it is seen that $\bar{\theta}_{i0}=0$.

In the hot end region, the governing equations are the same as Eqs. (74)–(76) except that Γ is replaced by $\Gamma+1$ and X is replaced by ξ. Applying the appropriate boundary conditions, the leading order temperature field in the hot end region is given by $\tilde{\theta}_{i0}=1$.

In order to apply conditions (72) and (73), $\hat{\theta}_{i0}$ is expanded in terms of the end region variables resulting in

$$\frac{3\mu^*+4h^*}{3\gamma_T^*h^*-6h^*}\frac{c_{11}}{Re}\ln\Gamma+\frac{3\mu^*+4h^*}{3\gamma_T^*h^*-6h^*}\frac{c_{11}}{Re}\left[\frac{\varepsilon X}{\Gamma}-\frac{1}{2}\left(\frac{\varepsilon X}{\Gamma}\right)^2+\cdots\right]+c_{11}^*=0, \tag{77}$$

$$\frac{3\mu^*+4h^*}{3\gamma_T^*h^*-6h^*}\frac{c_{11}}{Re}\ln(\Gamma+1)+\frac{3\mu^*+4h^*}{3\gamma_T^*h^*-6h^*}\frac{c_{11}}{Re}\times\left[-\frac{\varepsilon\xi}{1+\Gamma}-\frac{1}{2}\left(\frac{\varepsilon\xi}{1+\Gamma}\right)^2-\cdots\right]+c_{11}^*=1, \tag{78}$$

which gives

$$c_{11}=\frac{3\gamma_T^*h^*-6h^*}{3\mu^*+4h^*}\frac{Re}{\ln[(\Gamma+1)/\Gamma]}, \tag{79a}$$

$$c_{11}^*=\frac{\ln\Gamma}{\ln[\Gamma/(1+\Gamma)]}. \tag{79b}$$

The mismatch which occurs when to match at this order has to be accounted for when to match the solutions at higher order.

At $O(\varepsilon)$ the energy equation in the cold end region is simplified as

$$\frac{\partial^2\bar{\theta}_{11}}{\partial X^2}+\frac{\partial^2\bar{\theta}_{11}}{\partial Z^2}=0, \tag{80a}$$

$$\frac{\partial^2\bar{\theta}_{21}}{\partial X^2}+\frac{\partial^2\bar{\theta}_{21}}{\partial Z^2}=0. \tag{80b}$$

Integrating Eq. (80a) from $Z=-1$ to $Z=0$ and Eq. (80b) from $Z=0$ to $Z=h^*$, we have

$$\int_{-1}^{0}\frac{\partial^2\bar{\theta}_{11}}{\partial X^2}dZ+\left.\frac{\partial\bar{\theta}_{11}}{\partial Z}\right|_{Z=0}=0, \tag{81a}$$

$$\int_{0}^{h^*}\frac{\partial^2\bar{\theta}_{21}}{\partial X^2}dZ-\left.\frac{\partial\bar{\theta}_{21}}{\partial Z}\right|_{Z=0}=0. \tag{81b}$$

Combining Eqs. (81a) and (81b) and using the boundary condition at $Z=0:\ \partial\bar{\theta}_{11}/\partial Z=\lambda^*\partial\bar{\theta}_{21}/\partial Z$ yields

$$\int_{-1}^{0}\frac{\partial^2\bar{\theta}_{11}}{\partial X^2}dZ+\lambda^*\int_0^{h^*}\frac{\partial^2\bar{\theta}_{21}}{\partial X^2}dZ=0. \tag{82}$$

Integrating this twice with respect to X, and noting that $\bar{\theta}_{i1}=0$ at $X=0$ gives

$$\int_{-1}^{0}\bar{\theta}_{11}dZ+\lambda^*\int_0^{h^*}\bar{\theta}_{21}dZ=a_1X, \tag{83}$$

where a_1 is a constant of integration. This equation is valid everywhere in the cold end, and in particular, it is valid in the limit when the cold end approaches the core. According to the matching condition (72)

$$\bar{\theta}_{i1}\Longleftrightarrow\frac{3\mu^*+4h^*}{3\gamma_T^*h^*-6h^*}\frac{c_{11}}{Re}\frac{X}{\Gamma}+\frac{3\mu^*+4h^*}{3\gamma_T^*h^*-6h^*}\frac{c_{12}}{Re}\ln\Gamma+\frac{3\mu^*+4h^*}{3\gamma_T^*h^*-6h^*}\frac{c_{12}}{Re}\left[\frac{\varepsilon X}{\Gamma}-\frac{1}{2}\left(\frac{\varepsilon X}{\Gamma}\right)^2+\cdots\right]+c_{12}^*, \tag{84}$$

where the first term is the result of the mismatch at the leading order. Substituting this expansion into Eq. (83) and retaining only the leading order terms gives

$$(\lambda^*h^*+1)\left(\frac{3\mu^*+4h^*}{3\gamma_T^*h^*-6h^*}\frac{c_{11}}{Re}\frac{X}{\Gamma}+\frac{3\mu^*+4h^*}{3\gamma_T^*h^*-6h^*}\frac{c_{12}}{Re}\ln\Gamma+c_{12}^*\right)=a_1X. \tag{85}$$

Repeating the above analysis in the hot end region, we have

$$(\lambda^*h^*+1)\left(-\frac{3\mu^*+4h^*}{3\gamma_T^*h^*-6h^*}\frac{c_{11}}{Re}\frac{\xi}{\Gamma+1}+\frac{3\mu^*+4h^*}{3\gamma_T^*h^*-6h^*}\frac{c_{12}}{Re}\ln(\Gamma+1)+c_{12}^*\right)=a_2\xi, \tag{86}$$

where a_2 is an undetermined constant. Combining Eqs. (85) and (86) we have

$$a_1=\frac{3\mu^*+4h^*}{3\gamma_T^*h^*-6h^*}\frac{c_{11}}{Re}\frac{\lambda^*h^*+1}{\Gamma}, \tag{87}$$

$$a_2=-\frac{3\mu^*+4h^*}{3\gamma_T^*h^*-6h^*}\frac{c_{11}}{Re}\frac{\lambda^*h^*+1}{\Gamma+1}, \tag{88}$$

$$c_{12}=c_{12}^*=0. \tag{89}$$

At $O(\varepsilon^2)$ the energy equations in the cold end region can be written as

$$-\frac{Pr}{\Gamma+\varepsilon X}\frac{\partial\bar{\psi}_{10}}{\partial Z}\frac{3\mu^*+4h^*}{3\gamma_T^*h^*-6h^*}\frac{c_{11}}{Re}\frac{1}{\Gamma}=\frac{\partial^2\bar{\theta}_{12}}{\partial X^2}+\frac{\partial^2\bar{\theta}_{12}}{\partial Z^2}+\frac{3\mu^*+4h^*}{3\gamma_T^*h^*-6h^*}\frac{c_{11}}{Re}\frac{1}{\Gamma}\frac{1}{\Gamma+\varepsilon X}, \tag{90a}$$

$$-\frac{Pr}{\Gamma+\varepsilon X}\frac{\partial\bar{\psi}_{20}}{\partial Z}\frac{1}{\alpha^*}\frac{3\mu^*+4h^*}{3\gamma_T^*h^*-6h^*}\frac{c_{11}}{Re}\frac{1}{\Gamma}=\frac{\partial^2\bar{\theta}_{22}}{\partial X^2}+\frac{\partial^2\bar{\theta}_{22}}{\partial Z^2}+\frac{3\mu^*+4h^*}{3\gamma_T^*h^*-6h^*}\frac{c_{11}}{Re}\frac{1}{\Gamma}\frac{1}{\Gamma+\varepsilon X}, \tag{90b}$$

by first substituting for the known values of $\bar{\theta}_{i0}$ and $\bar{\theta}_{i1}$.

Integrating Eq. (90a) from $Z=-1$ to $Z=0$ and Eq. (90b) from $Z=0$ to $Z=h^*$ yields

$$\int_{-1}^{0}\frac{\partial^2\bar{\theta}_{12}}{\partial X^2}dZ+\left.\frac{\partial\bar{\theta}_{12}}{\partial Z}\right|_{Z=0}=-\frac{3\mu^*+4h^*}{3\gamma_T^*h^*-6h^*}\frac{c_{11}}{Re}\frac{1}{\Gamma}\frac{1}{\Gamma+\varepsilon X}, \tag{91a}$$

$$\int_0^{h^*}\frac{\partial^2\bar{\theta}_{22}}{\partial X^2}dZ-\left.\frac{\partial\bar{\theta}_{22}}{\partial Z}\right|_{Z=0}=-\frac{3\mu^*+4h^*}{3\gamma_T^*h^*-6h^*}\frac{c_{11}}{Re}\frac{h^*}{\Gamma}\frac{1}{\Gamma+\varepsilon X}. \tag{91b}$$

Combining Eqs. (91a) and (91b) and using the boundary condition at $Z=0:\partial\bar{\theta}_{12}/\partial Z=\lambda^*\partial\bar{\theta}_{22}/\partial Z$ yields

$$\int_{-1}^{0}\frac{\partial^2\bar{\theta}_{12}}{\partial X^2}dZ+\lambda^*\int_0^{h^*}\frac{\partial^2\bar{\theta}_{22}}{\partial X^2}dZ=-\frac{3\mu^*+4h^*}{3\gamma_T^*h^*-6h^*}\frac{c_{11}}{Re}\frac{1}{\Gamma}\frac{\lambda^*h^*+1}{\Gamma+\varepsilon X}. \tag{92}$$

Integrating Eq. (92) twice with respect to X and applying the appropriate boundary conditions yields

$$\int_{-1}^{0}\bar{\theta}_{12}dZ+\lambda^*\int_0^{h^*}\bar{\theta}_{22}dZ=-\frac{\lambda^*h^*+1}{2}\frac{3\mu^*+4h^*}{3\gamma_T^*h^*-6h^*}\frac{c_{11}}{Re}\frac{X^2}{\Gamma^2}+a_3X, \tag{93}$$

where a_3 is a constant of integration. The matching condition for $\bar{\theta}_{i2}$ is

$$\bar{\theta}_{i2}\Longleftrightarrow-\frac{1}{2}\frac{3\mu^*+4h^*}{3\gamma_T^*h^*-6h^*}\frac{c_{11}}{Re}\frac{X^2}{\Gamma^2}+\frac{3\mu^*+4h^*}{3\gamma_T^*h^*-6h^*}\frac{c_{13}}{Re}\ln\Gamma+\frac{3\mu^*+4h^*}{3\gamma_T^*h^*-6h^*}\frac{c_{13}}{Re}\left[\frac{\varepsilon X}{\Gamma}-\frac{1}{2}\left(\frac{\varepsilon X}{\Gamma}\right)^2+\cdots\right]+c_{13}^*, \tag{94}$$

where the first term is the result of the mismatch at the leading order. Applying this matching condition with Eq. (93) yields

$$(\lambda^*h^*+1)\left(-\frac{1}{2}\frac{3\mu^*+4h^*}{3\gamma_T^*h^*-6h^*}\frac{c_{11}}{Re}\frac{X^2}{\Gamma^2}+\frac{3\mu^*+4h^*}{3\gamma_T^*h^*-6h^*}\frac{c_{13}}{Re}\ln\Gamma+c_{13}^*\right)=-\frac{\lambda^*h^*+1}{2}\frac{3\mu^*+4h^*}{3\gamma_T^*h^*-6h^*}\frac{c_{11}}{Re}\frac{X^2}{\Gamma^2}+a_3X. \tag{95}$$

When the same analysis is repeated in the hot end region, the corresponding result is

$$(\lambda^*h^*+1)\left(-\frac{1}{2}\frac{3\mu^*+4h^*}{3\gamma_T^*h^*-6h^*}\frac{c_{11}}{Re}\frac{\xi^2}{(\Gamma+1)^2}+\frac{3\mu^*+4h^*}{3\gamma_T^*h^*-6h^*}\frac{c_{13}}{Re}\ln(\Gamma+1)+c_{13}^*\right)=-\frac{\lambda^*h^*+1}{2}\frac{3\mu^*+4h^*}{3\gamma_T^*h^*-6h^*}\frac{c_{11}}{Re}\frac{\xi^2}{(\Gamma+1)^2}+a_4\xi. \tag{96}$$

Combining the above two equations gives

$$c_{13}=c_{13}^*=a_3=a_4=0. \tag{97}$$

At $O(\varepsilon^3)$ the energy equation in the cold end region can be written as

$$\frac{3\mu^*+4h^*}{3\gamma_T^*h^*-6h^*}\frac{c_{11}}{Re}\frac{Pr}{\Gamma+\varepsilon X}\left(\frac{\partial\bar{\psi}_{10}}{\partial Z}\frac{X}{\Gamma^2}-\frac{\partial\bar{\psi}_{11}}{\partial Z}\frac{1}{\Gamma}\right)=\frac{\partial^2\bar{\theta}_{13}}{\partial X^2}+\frac{\partial^2\bar{\theta}_{13}}{\partial Z^2}-\frac{3\mu^*+4h^*}{3\gamma_T^*h^*-6h^*}\frac{c_{11}}{Re}\frac{1}{\Gamma^2}\frac{X}{\Gamma+\varepsilon X}, \tag{98a}$$

$$\frac{3\mu^*+4h^*}{3\gamma_T^*h^*-6h^*}\frac{1}{\alpha^*}\frac{c_{11}}{Re}\frac{Pr}{\Gamma+\varepsilon X}\left(\frac{\partial\bar{\psi}_{20}}{\partial Z}\frac{X}{\Gamma^2}-\frac{\partial\bar{\psi}_{21}}{\partial Z}\frac{1}{\Gamma}\right)=\frac{\partial^2\bar{\theta}_{23}}{\partial X^2}+\frac{\partial^2\bar{\theta}_{23}}{\partial Z^2}-\frac{3\mu^*+4h^*}{3\gamma_T^*h^*-6h^*}\frac{c_{11}}{Re}\frac{1}{\Gamma^2}\frac{X}{\Gamma+\varepsilon X}, \tag{98b}$$

by first substituting for the known values of $\bar{\theta}_{10}$, $\bar{\theta}_{11}$ and $\bar{\theta}_{12}$.

Integrating Eq. (98a) from $Z=-1$ to $Z=0$ and Eq. (98b) from $Z=0$ to $Z=h^*$ and applying the appropriate boundary conditions, we have

$$\int_{-1}^{0}\frac{\partial^2\bar{\theta}_{13}}{\partial X^2}dZ+\left.\frac{\partial\bar{\theta}_{13}}{\partial Z}\right|_{Z=0}=\frac{3\mu^*+4h^*}{3\gamma_T^*h^*-6h^*}\frac{c_{11}}{Re}\frac{1}{\Gamma^2}\frac{X}{\Gamma+\varepsilon X}, \tag{99a}$$

$$\int_0^{h^*}\frac{\partial^2\bar{\theta}_{23}}{\partial X^2}dZ-\left.\frac{\partial\bar{\theta}_{23}}{\partial Z}\right|_{Z=0}=\frac{3\mu^*+4h^*}{3\gamma_T^*h^*-6h^*}\frac{c_{11}}{Re}\frac{h^*}{\Gamma^2}\frac{X}{\Gamma+\varepsilon X}. \tag{99b}$$

Combining Eqs. (99a) and (99b) and using the boundary condition at $Z=0:\partial\bar{\theta}_{13}/\partial Z=\lambda^*\partial\bar{\theta}_{23}/\partial Z$ yields

$$\int_{-1}^{0}\frac{\partial^2\bar{\theta}_{13}}{\partial X^2}dZ+\lambda^*\int_0^{h^*}\frac{\partial^2\bar{\theta}_{23}}{\partial X^2}dZ=\frac{3\mu^*+4h^*}{3\gamma_T^*h^*-6h^*}\frac{c_{11}}{Re}\frac{\lambda^*h^*+1}{\Gamma^2}\frac{X}{\Gamma+\varepsilon X}. \tag{100}$$

Integrating Eq. (100) twice with respect to X and applying the appropriate boundary conditions yields

$$\int_{-1}^{0}\bar{\theta}_{13}dZ+\lambda^*\int_0^{h^*}\bar{\theta}_{23}dZ=\frac{\lambda^*h^*+1}{6}\frac{3\mu^*+4h^*}{3\gamma_T^*h^*-6h^*}\frac{c_{11}}{Re}\frac{X^3}{\Gamma^3}+b_3X, \quad (101)$$

where b_3 is a constant of integration. The matching condition for $\bar{\theta}_{i3}$ is

$$\bar{\theta}_{13}\Longleftrightarrow\frac{1}{6}\frac{3\mu^*+4h^*}{3\gamma_T^*h^*-6h^*}\frac{c_{11}}{Re}\frac{X^3}{\Gamma^3}+\frac{M}{\Gamma^2}\left(\frac{Z^4}{24}+\frac{Z^3}{9}+\frac{Z^2}{12}-\frac{1}{120}\frac{1}{\lambda^*h^*+1}-\frac{3Ah^{*4}+15Bh^{*3}+10h^{*2}}{360}\frac{\lambda^*h^*}{\lambda^*h^*+1}\frac{1}{\alpha^*}\right)+a_3'\ln\Gamma+d_3, \quad (102)$$

$$\bar{\theta}_{23}\Longleftrightarrow\frac{1}{6}\frac{3\mu^*+4h^*}{3\gamma_T^*h^*-6h^*}\frac{c_{11}}{Re}\frac{X^3}{\Gamma^3}+\frac{1}{\alpha^*}\frac{M}{\Gamma^2}\left(\frac{Az^4}{24}+\frac{Bz^3}{6}+\frac{z^2}{12}-\frac{1}{120}\frac{\alpha^*}{\lambda^*h^*+1}-\frac{3Ah^{*4}+15Bh^{*3}+10h^{*2}}{360}\frac{\lambda^*h^*}{\lambda^*h^*+1}\right)+a_3'\ln(\Gamma+\hat{x})+d_3, \quad (103)$$

where the first terms are the result of the mismatch at the leading order. Applying this matching condition with Eq. (101) yields

$$(\lambda^*h^*+1)\left(\frac{1}{6}\frac{3\mu^*+4h^*}{3\gamma_T^*h^*-6h^*}\frac{c_{11}}{Re}\frac{X^3}{\Gamma^3}+a_3'\ln\Gamma+d_3\right)=\frac{\lambda^*h^*+1}{6}\frac{3\mu^*+4h^*}{3\gamma_T^*h^*-6h^*}\frac{c_{11}}{Re}\frac{X^3}{\Gamma^3}+b_3X. \quad (104)$$

When the same analysis is repeated in the hot end region, the corresponding result is

$$(\lambda^*h^*+1)\left(\frac{1}{6}\frac{3\mu^*+4h^*}{3\gamma_T^*h^*-6h^*}\frac{c_{11}}{Re}\frac{\xi^3}{(\Gamma+1)^3}+a_3'\ln(\Gamma+1)+d_3\right)=\frac{\lambda^*h^*+1}{6}\frac{3\mu^*+4h^*}{3\gamma_T^*h^*-6h^*}\frac{c_{11}}{Re}\frac{\xi^3}{(\Gamma+1)^3}+b_4\xi. \quad (105)$$

Combining the above two equations gives

$$a_3'=d_3=b_3=b_4=0. \quad (106)$$

5. Asymptotic solution

Substituting Eqs. (39), (44), (45), (58), (59), (62), (65) and (70) into Eq. (28) and noticing Eqs. (66), (79), (89), (97) and (106), we can obtain the asymptotic solutions of thermocapillary convection in the core region as follows

$$\theta_1\approx\theta_{10}+\varepsilon\theta_{11}+\varepsilon^2\theta_{12}+\varepsilon^3\theta_{13}=\frac{\ln\frac{\Gamma}{\Gamma+\varepsilon X}}{\ln\frac{\Gamma}{\Gamma+1}}+\frac{3\gamma_T^*h^*-6h^*}{3\mu^*+4h^*}\frac{PrRe}{\left(\ln\frac{\Gamma+1}{\Gamma}\right)^2}\frac{\varepsilon^3}{(\Gamma+\varepsilon X)^2}\left(\frac{Z^4}{24}+\frac{Z^3}{9}+\frac{Z^2}{12}-\frac{1}{120}\frac{1}{\lambda^*h^*+1}-\frac{3Ah^{*4}+15Bh^{*3}+10h^{*2}}{360}\frac{\lambda^*h^*}{\lambda^*h^*+1}\frac{1}{\alpha^*}\right), \quad (107)$$

$$\theta_2\approx\theta_{20}+\varepsilon\theta_{21}+\varepsilon^2\theta_{22}+\varepsilon^3\theta_{23}=\frac{\ln\frac{\Gamma}{\Gamma+\varepsilon X}}{\ln\frac{\Gamma}{\Gamma+1}}+\frac{3\gamma_T^*h^*-6h^*}{3\mu^*+4h^*}\frac{1}{\alpha^*}\frac{PrRe}{\left(\ln\frac{\Gamma+1}{\Gamma}\right)^2}\frac{\varepsilon^3}{(\Gamma+\varepsilon X)^2}\left(\frac{AZ^4}{24}+\frac{BZ^3}{6}+\frac{Z^2}{12}-\frac{1}{120}\frac{\alpha^*}{\lambda^*h^*+1}-\frac{3Ah^{*4}+15Bh^{*3}+10h^{*2}}{360}\frac{\lambda^*h^*}{\lambda^*h^*+1}\right), \quad (108)$$

$$\psi_1\approx\psi_{10}+\varepsilon\psi_{11}+\varepsilon^2\psi_{12}+\varepsilon^3\psi_{13}=\frac{3\gamma_T^*h^*-6h^*}{3\mu^*+4h^*}\frac{Re}{\ln\frac{\Gamma}{\Gamma+1}}\left(\frac{Z^3}{6}+\frac{Z^2}{3}+\frac{Z}{6}\right), \quad (109)$$

$$\psi_2\approx\psi_{20}+\varepsilon\psi_{21}+\varepsilon^2\psi_{22}+\varepsilon^3\psi_{23}=\frac{3\gamma_T^*h^*-6h^*}{3\mu^*+4h^*}\frac{Re}{\ln\frac{\Gamma}{\Gamma+1}}\left(\frac{AZ^3}{6}+\frac{BZ^2}{2}+\frac{Z}{6}\right). \quad (110)$$

Applying the equation $U=-\frac{1}{R}\frac{\partial\psi}{\partial Z}$ yields

$$U_1=\frac{3\gamma_T^*h^*-6h^*}{3\mu^*+4h^*}\frac{\varepsilon}{\Gamma+\varepsilon X}\frac{Re}{\ln(1+1/\Gamma)}\left(\frac{Z^2}{2}+\frac{2Z}{3}+\frac{1}{6}\right), \quad (111)$$

$$U_2=\frac{3\gamma_T^*h^*-6h^*}{3\mu^*+4h^*}\frac{\varepsilon}{\Gamma+\varepsilon X}\frac{Re}{\ln(1+1/\Gamma)}\left(A\frac{Z^2}{2}+BZ+\frac{1}{6}\right). \quad (112)$$

If $\Gamma\to\infty$, we have

$$\lim_{\Gamma\to\infty}\theta_1=\varepsilon X+\frac{3\gamma_T^*h^*-6h^*}{3\mu^*+4h^*}PrRe\varepsilon^3\left(\frac{Z^4}{24}+\frac{Z^3}{9}+\frac{Z^2}{12}-\frac{1}{120}\frac{1}{\lambda^*h^*+1}-\frac{3Ah^{*4}+15Bh^{*3}+10h^{*2}}{360}\frac{\lambda^*h^*}{\lambda^*h^*+1}\frac{1}{\alpha^*}\right), \quad (113)$$

$$\lim_{\Gamma\to\infty}\theta_2=\varepsilon X+\frac{3\gamma_T^*h^*-6h^*}{3\mu^*+4h^*}\frac{1}{\alpha^*}PrRe\varepsilon^3\left(\frac{AZ^4}{24}+\frac{BZ^3}{6}+\frac{Z^2}{12}-\frac{1}{120}\frac{\alpha^*}{\lambda^*h^*+1}-\frac{3Ah^{*4}+15Bh^{*3}+10h^{*2}}{360}\frac{\lambda^*h^*}{\lambda^*h^*+1}\right), \quad (114)$$

$$\lim_{\Gamma\to\infty}U_1=\frac{3\gamma_T^*h^*-6h^*}{3\mu^*+4h^*}\varepsilon Re\left(\frac{Z^2}{2}+\frac{2Z}{3}+\frac{1}{6}\right), \quad (115)$$

$$\lim_{\Gamma\to\infty}U_2=\frac{3\gamma_T^*h^*-6h^*}{3\mu^*+4h^*}\varepsilon Re\left(A\frac{Z^2}{2}+BZ+\frac{1}{6}\right). \quad (116)$$

In this case, thin annular pool approaches to thin two-dimensional slot. Therefore, Eqs. (113)–(116) are the same as the results obtained by Doi and Koster [12].

It is found that the value of U_1 in Eq. (111) becomes zero at $\gamma_T^*=2$, therefore, the fluid motion halts in the lower liquid layer. This is a very attractive feature of the thermocapillary convection in two immiscible liquid layers. At same time, we find other two conditions to stop fluid motion in the lower liquid layer, which are $\mu^*\to\infty$ and $h^*\to0$. The same situations are also found in two-dimensional slot by Doi and Koster [12].

6. Numerical experiments and comparison

Numerical experiments are carried out to compare simulation results with the asymptotic solution of the steady two-dimensional thermocapillary convection. The B_2O_3/GaAs system is used for both the numerical simulation and the asymptotic solution. The fundamental equations are discretized by the finite-difference method. The modified central approximation is applied to the diffusion terms while the QUICK scheme is used for the convective terms. The SIMPLEC algorithm is adopted to correct simultaneously the pressure and the velocities. In this study, nonuniform staggered grid of $120^r\times60^z$ is chosen for all cases. The validation of the code for the thermocapillary flow simulation was performed in our previous works [27], and there is no need to repeat here. $Re=10^6$ and 10^7, $\Gamma=0.25$, $\varepsilon=0.05$ and 0.1, $h^*=0.5$, 1.0 and 2.0 are used in this work and the thermophysical properties of B_2O_3 and GaAs are listed in Table 1.

Fig. 2 shows the radial distributions of radial velocity at the free surface and the interface at $\varepsilon=0.05$, $h^*=1$ and $Re=10^7$. Any radial temperature difference produces a surface tension gradient along the free surface and an interface tension gradient along the

Table 1
Physical properties.

Gallium arsenide
Density, $\rho_1 = 5720\ \mathrm{kg/m^3}$
Dynamic viscosity, $\mu_1 = 2.79 \times 10^{-3}\ \mathrm{kg/m\ s}$
Specific heat, $c_{p1} = 434\ \mathrm{J/kg\ K}$
Thermal conductivity, $\lambda_1 = 17.8\ \mathrm{W/m\ K}$
Interface tension temperature coefficient, $\gamma_{T,1} = -1.2 \times 10^{-3}\ \mathrm{N/m\ K}$
Boron oxide
Density, $\rho_2 = 1648\ \mathrm{kg/m^3}$
Dynamic viscosity, $\mu_2 = 3.9\ \mathrm{kg/m\ s}$
Specific heat, $c_{p2} = 1830\ \mathrm{J/kg\ K}$
Thermal conductivity, $\lambda_2 = 2.0\ \mathrm{W/m\ K}$
Surface tension temperature coefficient, $\gamma_{T,2} = 3.57 \times 10^{-5}\ \mathrm{N/m\ K}$

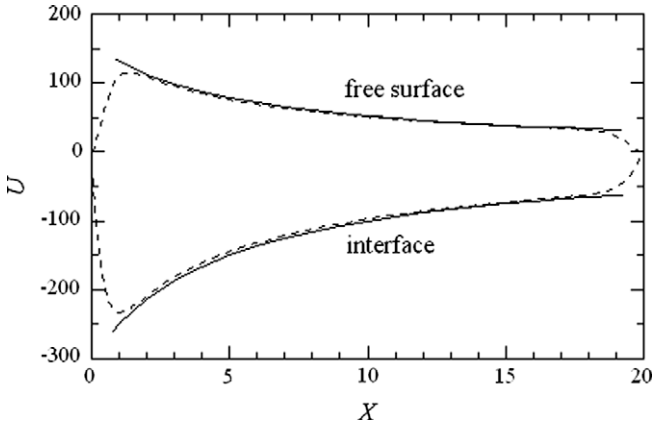

Fig. 2. The radial distributions of radial velocity at the free surface and the interface at $Re = 10^7$, $\varepsilon = 0.05$ and $h^* = 1.0$. Solid line: asymptotic solution; dotted line: simulation result.

interface, and the thermocapillary effect induces the convective motions in the two layers. In the present case, the thermocapillary forces act in opposite directions at the free surface and the interface surface. Thus there is a counterclockwise circulation in lower liquid layer 1 and a clockwise circulation in the upper liquid layer 2. The free surface fluid flows from the cold wall toward the hot wall, while the interface flow is from the hot wall toward the cold wall. The maximum radial velocities at the free surface and the interface both locate near the inner cylinder. For all case the temperature distribution in the radial direction is almost independent on the presence of the flow, which approaches the conductivity temperature distribution at small thermocapillary Reynolds number. Fig. 3 gives vertical distributions of the radial velocity in the middle part at $Re = 10^7$, $h^* = 1$, $\varepsilon = 0.05$ and 0.1. For both cases, the simulation results of the radial velocity are almost same as the asymptotical solution. In the asymptotical solutions, the terms of $o(\varepsilon^3)$ are neglected. Therefore, the error between the asymptotical solutions and the simulation results increases with the increase of the aspect ratio ε. It is found that the asymptotical solutions are not suitable near the inner cylinder and outer cylinder, for the end effects are not considered in the present analysis. Near the inner cylinder and outer cylinder, the flow structure and temperature distribution can only be obtained by a numerical method, as shown by Sen and Davis [25].

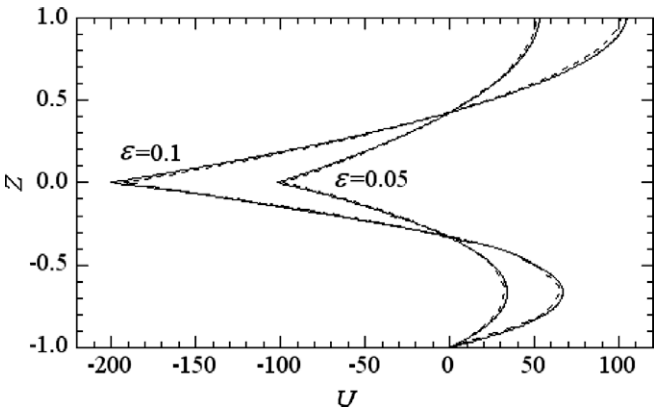

Fig. 3. Distribution of radial velocity in the middle part as a function of Z for the case of $Re = 10^7$. Solid line: asymptotic solution; dotted line: simulation result.

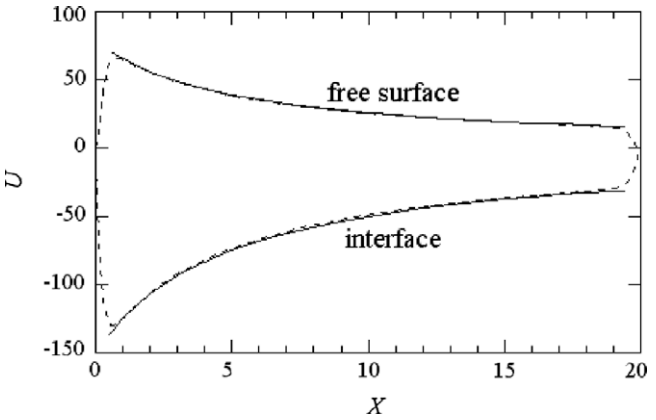

Fig. 4. The radial distributions of radial velocity at the free surface and the interface for the case of $\varepsilon = 0.05$ at $Re = 10^7$ and $h^* = 0.5$. Solid line: asymptotic solution; dotted line: simulation result.

In order to estimate the effect of the thickness ratio of the two layers, we also calculate the radial distributions of radial velocity at the free surface and the interface for the cases of $h^* = 0.5$ and 2, as shown in Figs. 4 and 5, respectively. It is found that the error between the asymptotical solutions and the simulation results in the cases of $h^* = 0.5$ is smaller than that in the case of $h^* = 2$. At $Re = 10^7$, the asymptotical solutions at $h^* = 2$ is invalidity. It means the range of validity of the asymptotical solutions decreases gradually with the increase of the thickness ratio of the two layers.

7. Conclusions

Approximate solutions of thermocapillary convection under microgravity condition in a differentially heated annular pool of the two-layer system are obtained in the core region in the limit as the aspect ratio goes to zero. And two-dimensional numerical

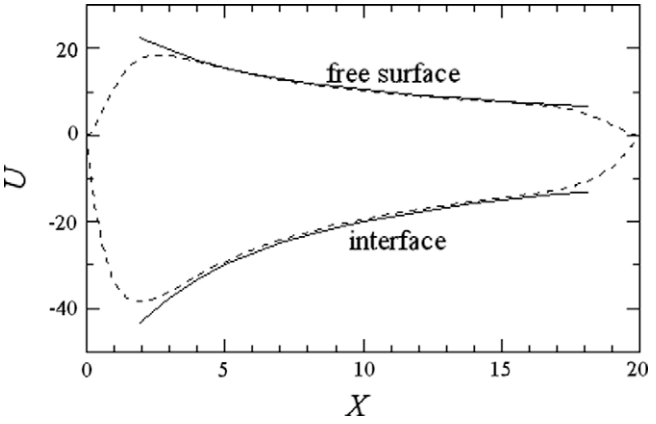

Fig. 5. The radial distributions of radial velocity at the free surface and the interface for the case of $\varepsilon = 0.05$ at $Re = 10^6$ and $h^* = 2.0$. Solid line: asymptotic solution; dotted line: simulation result.

simulation is also performed under the same conditions. The results show that the asymptotical solutions of the temperature and the velocity in the core region have a good agreement with the simulation results. The error between the asymptotical solutions and the simulation results increases with the increase of the aspect ratio and the thickness ratio of the two layers. However, the asymptotical solutions are not suitable near the inner cylinder and outer cylinder, for the end effects are not considered in the present analysis.

Acknowledgment

This work is supported by National Natural Science Foundation of China (Grant No. 50776102).

References

[1] J.S. Walker, D. Henry, H. Ben Hadid, Magnetic stabilization of the buoyant convection in the liquid-encapsulated Czochralski process, J. Cryst. Growth 243 (2002) 108–116.
[2] J.L. Morton, N. Ma, D.F. Bliss, G.G. Bryant, Magnetic field effects during liquid-encapsulated Czochralski growth of doped photonic semiconductor crystals, J. Cryst. Growth 250 (2003) 174–182.
[3] M. Jurisch, F. Borner, T. Bunger, S. Eichler, T. Flade, U. Kretzer, A. Kohler, J. Stenzenberger, B. Weinert, LEC- and VGF-growth of SI GaAs single crystals – recent developments and current issues, J. Cryst. Growth 275 (2005) 283–291.
[4] P. Georis, M. Hennenberg, I.B. Simanovskii, A. Nepomniaschy, I.I. Wertgeim, J.C. Legros, Thermocapillary convection in a multilayer system, Phys. Fluids A 5 (1993) 1575–1582.
[5] A.A. Nepomnyashchy, I.B. Simanovskii, Combined action of anticonvective and thermocapillary mechanisms of instability, Phys. Fluids 14 (2002) 3855–3867.
[6] Q.S. Liu, B.H. Zhou, R. Liu, H. Nguyen-Thi, B. Billia, Oscillatory instabilities of two-layer Rayleigh–Marangoni–Benard convection, Acta Astronaut. 59 (2006) 40–45.
[7] S. Punjabi, K. Muralidhar, P.K. Panigrahi, Influence of layer height on thermal buoyancy convection in a system with two superposed fluids confined in a parallelepipedic cavity, Fluid Dyn. Mater. Process 2 (2006) 95–105.
[8] S. Sahu, K. Muralidhar, P.K. Panigrahi, Interface deformation and convective transport in horizontal differentially heated air–oil layers, Fluid Dyn. Mater. Process 3 (2007) 265–286.
[9] T. Boeck, A. Nepomnyashchy, I. Simanovskii, Three-dimensional simulations of water–mercury anticonvection, Fluid Dyn. Mater. Process 4 (2008) 11–20.
[10] D. Villers, J.K. Platten, Thermal convection in superposed immiscible liquid layers, Appl. Sci. Res. 45 (1988) 145–152.
[11] D. Villers, J.K. Platten, Influence of interfacial tension gradients on thermal convection in two superposed immiscible liquid layers, Appl. Sci. Res. 47 (1990) 177–202.
[12] T. Doi, J.N. Koster, Thermocapillary convection in two immiscible liquid layers with free surface, Phys. Fluids A 5 (1993) 1914–1927.
[13] Q.S. Liu, G. Chen, B. Roux, Thermogravitational and thermocapillary convection in a cavity containing two superposed immiscible liquid layers, Int. J. Heat Mass Transfer 36 (1993) 101–117.
[14] Q.S. Liu, B. Roux, M.G. Velarde, Thermocapillary convection in two-layers system, Int. J. Heat Mass Transfer 41 (1998) 1499–1511.
[15] A.A. Nepomnyashchy, I.B. Simanovskii, L.M. Braverman, Spiral thermocapillary flows in two-layer systems, Eur. J. Mech. B/Fluids 18 (1999) 1005–1026.
[16] S. Madruga, C. Perez-Garcia, G. Lebon, Convective instabilities in two superposed horizontal liquid layers heated laterally, Phys. Rev. E 68 (2003) 041607.
[17] A.A. Nepomnyashchy, I.B. Simanovskii, Convective flows in a two-layer system with a temperature gradient along the interface, Phys. Fluids 18 (2006) 032105.
[18] N.R. Gupta, H. Haj-Hariri, A. Borhanc, Thermocapillary flow in double-layer fluid structures: an effective single-layer model, J. Colloid Interface Sci. 293 (2006) 158–171.
[19] N.R. Gupta, H. Haj-Hariri, A. Borhanc, Thermocapillary convection in double-layer fluid structures within a two-dimensional open cavity, J. Colloid Interface Sci. 315 (2007) 237–247.
[20] A.A. Nepomnyashchy, I.B. Simanovskii, Nonlinear stability of buoyancy-thermocapillary flows in two-layer systems with a temperature gradient along the interface, J. Phys. Conf. Ser. 64 (2007) 012017.
[21] Q.M. Chang, J. Iwan, D. Alexander, Study of Marangoni-natural convection in a two-layer liquid system with density inversion using a lattice Boltzmann model, Phys. Fluids 19 (2007) 102107.
[22] D.E. Cormack, L.G. Leal, J. Imberger, Natural convection in a shallow cavity with differentially heated end walls. Part 1. Asymptotic theory, J. Fluid Mech. 65 (1974) 209–229.
[23] G.P. Merker, L.G. Leal, Natural convection in a shallow annular cavity, Int. J. Heat Mass Transfer 23 (1980) 677–686.
[24] D.M. Leppinen, Natural convection in a shallow cylindrical annuli, Int. J. Heat Mass Transfer 45 (2002) 2967–2981.
[25] A.K. Sen, S.H. Davis, Steady thermocapillary flows in two-dimensional slots, J. Fluid Mech. 121 (1982) 163–186.
[26] Y.R. Li, X.X. Zhao, S.Y. Wu, L. Peng, Asymptotic solution of thermocapillary convection in a thin annular pool of silicon melt, Phys. Fluids 20 (2008) 082107.
[27] Y.R. Li, W.J. Zhang, S.C. Wang, Two-dimensional numerical simulation of thermocapillary convection in annular two-layer system, Microgravity Sci. Technol. 20 (2008) 313–317.